


## Article

# Lodged Sugarcane/Crop Dividers Interaction: Analysis of Robotic Sugarcane Harvester in Agriculture via a Rigid-Flexible Coupled Simulation Method

Qingqing Wang<sup>1,2</sup>, Qianwei Zhang<sup>1</sup>, Yin Zhang<sup>1</sup>, Guoan Zhou<sup>1</sup>, Zhiqiang Li<sup>1</sup> and Liqing Chen<sup>1,2,\*</sup> 

<sup>1</sup> College of Engineering, Anhui Agricultural University, Hefei 230036, China; qqwang@stu.ahau.edu.cn (Q.W.); qianweizhang@stu.ahau.edu.cn (Q.Z.); zhangyin@stu.ahau.edu.cn (Y.Z.); zga@stu.ahau.edu.cn (G.Z.); ZhiQiangLi@ahau.edu.cn (Z.L.)

<sup>2</sup> Anhui Province Engineering Laboratory of Intelligent Agricultural Machinery and Equipment, Hefei 230036, China

\* Correspondence: lqchen@ahau.edu.cn

**Abstract:** As a critical component of the sugarcane harvester, the primary function of the crop dividers is to lift the lodged sugarcane (LS) and reduce the loss rate of the sugarcane harvest. In this study, a rigid-flexible coupling simulation method is proposed to improve the lifting efficiency of the crop dividers on severely LS and analyze the nature of interaction between the sugarcane stalk and the crop dividers. The model's accuracy was verified using field experiments, and the operational performance of the crop dividers on sugarcane in different lodging postures was investigated. The results showed that the curve of the vertical height of the center (VHC) fluctuated more and slipped with highest frequency during the lifting process of side and forward LS. The speed of VHC was fastest during the lifting operation of side LS. The effect of side angle on the lifting effect of sugarcane was significant; the qualified values of the VHC of sugarcane being lifted in different lodged postures were: side and reverse lodged > side lodged > side and forward lodged. The coupling method and experimental results described in this paper can provide guidance for the optimal design and field operation of the crop dividers.

**Keywords:** crop dividers; rigid-flexible coupling; side angles; lodged sugarcane (LS); vertical height of the center (VHC)



**Citation:** Wang, Q.; Zhang, Q.; Zhang, Y.; Zhou, G.; Li, Z.; Chen, L. Lodged Sugarcane/Crop Dividers Interaction: Analysis of Robotic Sugarcane Harvester in Agriculture via a Rigid-Flexible Coupled Simulation Method. *Actuators* **2022**, *11*, 23. <https://doi.org/10.3390/act11010023>

Academic Editor: Xiaoqi Chen

Received: 29 November 2021

Accepted: 10 January 2022

Published: 13 January 2022

**Publisher's Note:** MDPI stays neutral with regard to jurisdictional claims in published maps and institutional affiliations.



**Copyright:** © 2022 by the authors. Licensee MDPI, Basel, Switzerland. This article is an open access article distributed under the terms and conditions of the Creative Commons Attribution (CC BY) license (<https://creativecommons.org/licenses/by/4.0/>).

## 1. Introduction

As the primary raw material for sugar production, sugarcane is mainly grown in tropical and subtropical regions [1–4] and is an essential economic pillar industry in many countries and regions [5,6]. The use of mechanized sugarcane harvesting can greatly improve efficiency and, with the rapid development of smart agriculture, the development of intelligent harvesting machinery has become a focus for research in recent years. For sugarcane harvesters, Kallaya et al. provide a reasonable reference method for planning the driving route of harvesters to reduce the loss rate of sugarcane mechanical harvesting [7]. In [8], the required power requirements and field performance of sugarcane harvester components in operation were quantified. Lucas et al. evaluated the quality of mechanically harvested sugarcane by three different cropping methods using statistical methods [9].

The planting area of sugarcane in China ranks third globally, mainly in provinces such as Guangxi, Guangdong and Hainan [10,11]. The planting of sugarcane in this area is mainly based on slopes and hills. Due to the influence of typhoons and the monsoon climate every year, sugarcane will lodged to different degrees during the growth process, as shown in Figure 1 [12,13]. It is worth noting that lodged sugarcane (LS) brings difficulties to mechanized harvesting and increases the loss rate of mechanical harvesting, bringing economic losses to farmers. In the mechanized harvesting process, if the LS cannot be

raised to a certain height, this will cause the knife to cut the sugarcane multiple times and increase the root damage rate [14,15]. More importantly, this will reduce the yield and seriously affect the sugarcane's sprouting growth in the coming year [16,17]. Therefore, the design of the crop dividers of the sugarcane harvester is particularly important.



**Figure 1.** LS after typhoon.

As an essential component of the sugarcane harvester, the sugarcane supporting mechanism is mainly used to lift the sugarcane to a certain height to facilitate the work of the cutting mechanism. It is mainly divided into spiral and finger chain types [18]. Many scholars at home and abroad have carried out research on this. For the finger chain type, Mou et al. carried out simulation analysis and bench test research on the problems of missing support and lift lodging angle parameters [19]. At present, sugarcane harvesters on the market mostly still employ the installation of spiral crop dividers, and interested scholars have carried out a series of studies into this [20]. In [18,20], the effects of different lodging angles, forward velocity (FV), scrolls speed and the ground clearance of the crop divider toes on lifting performance were investigated in a field experiment. It was concluded that it is necessary to improve the operational performance of the crop divider for different inversions of sugarcane. Gao et al. established a mechanical model of sugarcane growth in the field and analyzed the interaction process between the lifting scrolls and the sugarcane [21,22]. Song et al. designed a test device for the crop divider. They discussed the influence of the spiral scroll speed, the crop divider's FV, and the helical inclination angle on the sugarcane lifting effect, and the impact of friction and lifting performance [23–25]. In [26], unequal pitch crop dividers were designed, and a physical model was constructed to verify their feasibility through computer simulation. Xie et al. created combined crop dividers consisting of a spiral scroll and a finger chain and conducted an experimental study in a soil trough [27]. The above shows that most of the research on the spiral crop dividers explores the influence of different structural parameters and motion parameters on performance, which provides a basis for improving the operational performance of the crop dividers. However, most of the above studies have focused on moderately LS. Severely LS presents problems, such as being close to the ground, difficulty in lifting, and low efficiency compared to medium lodging, which are the main reasons for the high rate of cut breakage [23]. Therefore, harvesting severely LS is still an unsolved problem; analysis of the law governing interaction between sugarcane in different lodged postures and the crop dividers is key to solving this problem.

The analysis method using rigid-flexible coupling can accurately describe the interactions between components and has been applied in many fields. For example, Duan et al. used a rigid-flexible coupling simulation method to analyze the transmission error

of gear meshing at the system level [28]. Xia et al. studied the interaction effect between the rigid open mechanism and the flexible ordinary multi-layer fruit paper bag. They provided valuable guidance for the operating parameters of the rigid mechanism [29]. Liu et al. conducted simulation experiments on the proposed 3-5R parallel mechanism using the rigid-flexible coupling method and verified the feasibility of the mechanism [30]. During contact between severely LS and the crop dividers, the sugarcane will be deformed by the collision force, so the interaction between the LS and the crop divider mechanism relates to the study of rigid-flexible coupling dynamics. Based on the above analysis, this paper proposes a rigid-flexible coupling dynamics approach based on interaction analysis between the severely LS and the crop dividers of the harvester.

In this paper, a rigid-flexible coupling dynamics simulation method of LS and crop dividers is proposed. A coupled simulation model of the spiral crop dividers and LS based on ADAMS software is established, and the accuracy of the model is verified using field tests. Taking LS as the research object, simulation experiments of different forward speeds were carried out, and the speed and height change relationships of sugarcane in the lifting process with different postures were analyzed. In addition, the slipping frequency and maximum vertical height of centroid (VHC) of the sugarcane during the lifting process were compared. The experimental results provide a reference for the operation mode between the harvester and the LS.

The remainder of this paper is organized as follows. Section 2 briefly analyzes the kinematic characteristics of the spiral crop dividers. Section 3 describes the establishment of the simulation model of the crop dividers and sugarcane and explains the experimental design plan and evaluation index. Section 4 first verifies the accuracy of the simulation model, based on which the interaction between LS/spiral crop dividers is analyzed and the experimental results are discussed. The Conclusions section is presented in Section 5.

## 2. Working Principle of Spiral Crop Dividers

### 2.1. Working Principle and Components

The sugarcane harvester is mainly composed of topper, crop dividers, base cutter, feed rollers, chopper rollers, extractor and collection bin, as shown in Figure 2. During the harvester's operation, the topper cuts the top of the sugarcane, the crop dividers lift the LS to a certain height, the base cutter cuts the sugarcane roots then conveys it to the feed devices. The chopper rollers cut the whole sugarcane into segments. Finally, the extractor device removes impurities, and the sugarcane segments are put into the collection bin [31].

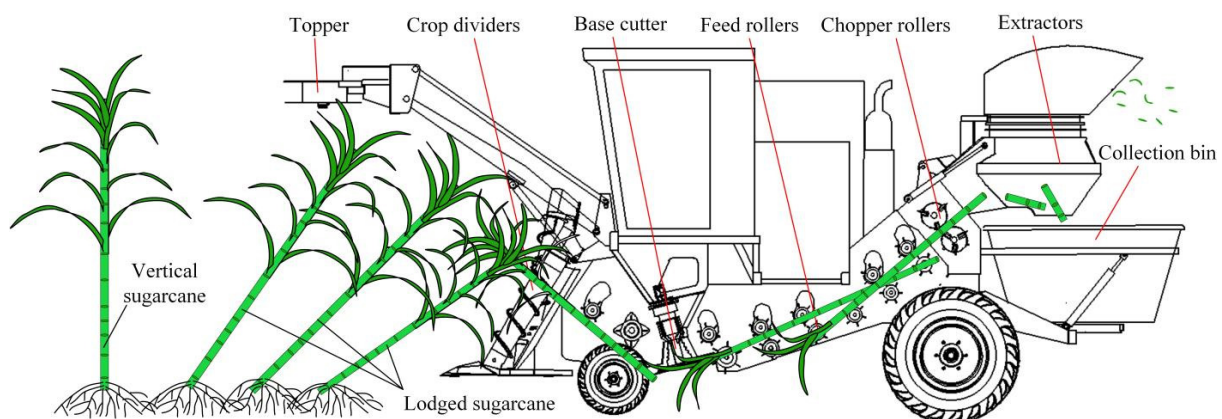


**Figure 2.** Sugarcane harvester component parts.

The crop dividers are mainly comprised of the bracket, lifting scrolls, divider scrolls, divider toes, hydraulic motor, etc. Lifting scrolls and divider scrolls are the main components of the crop dividers, which are usually conical in shape, both with spiral guide tubes and spiral guide plates. Each harvester is installed with two crop dividers, on the left and right sides of the inlet, in a symmetrical installation, as in Figure 3.

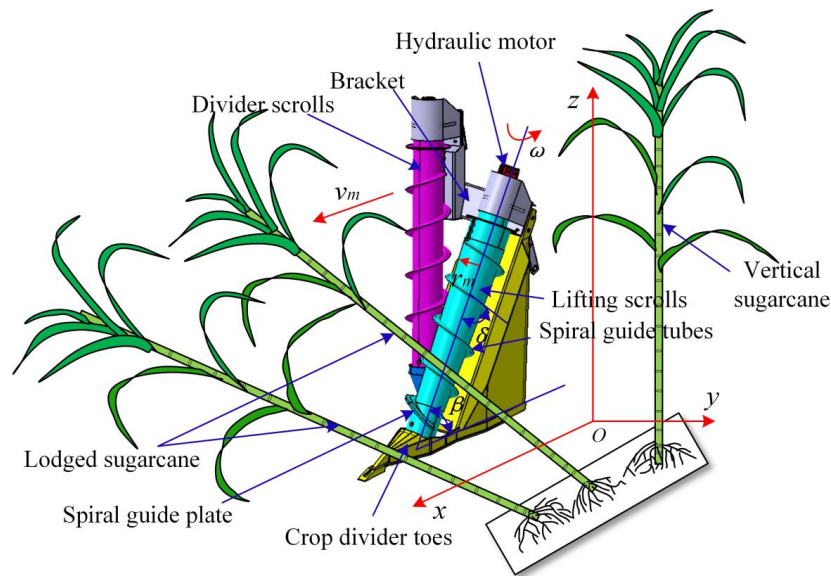


**Figure 3.** Working principle and components of spiral crop dividers.

During operation, the lifting scrolls and the divider scrolls rotate around their central axes. As the harvester progresses, the LS gradually rises along with the lifting scrolls and gathers in the middle of the crop row. The function of the divider scrolls is to lift and branch the adjacent rows of LS. After the LS is lifted to a certain height, the base cutter cuts sections from the root of the sugarcane and then transports it to the feed rollers [5].

According to Figure 3, it can be observed that during the interaction between the LS and the lifting scrolls, the contact position is a moving point that rises along the spiral guide tubes. The tangent velocity of the moving point along the lifting scrolls is:

$$v_n = \omega r_m \quad (1)$$

where  $v_n$  is the tangent velocity of the contact point, with the unit of m/s,  $\omega$  is the angular velocity of the lifting scrolls, with the unit of r/min, and  $r_m$  is the radius of the lifting scrolls, with the unit of m. The moving point moves in three-dimensional space, and its position equations at different moments are:

$$\begin{cases} X = v_n t \cos \beta \cos \delta - v_m t \\ Y = v_n t \cos \beta \sin \delta \\ Z = v_n t \sin \delta \end{cases} \quad (2)$$

where  $X$  is the displacement of the contact point in the X-axis direction, with the unit of m,  $t$  is time, with the unit of s,  $\beta$  is the angle between the lifting scrolls and the horizontal plane, with the unit of  $^\circ$ ,  $\delta$  is the inclination angle of the spiral guide tubes, with the unit of  $^\circ$ ,  $Y$  is the displacement of the contact point in the Y-axis direction, with the unit of m, and  $Z$  is the displacement of the contact point in the Z-axis direction, with the unit of m. Due to the radius of the lifting scrolls being variable, with the rotation of the lifting scrolls and the operation of the harvester, the velocity equation of the contact point is:

$$\begin{cases} v_x = \frac{dX}{dt} = v_n \cos \beta \cos \delta - v_m \\ v_y = \frac{dY}{dt} = v_n \cos \beta \sin \delta \\ v_z = \frac{dZ}{dt} = v_n \sin \delta \end{cases} \quad (3)$$

where  $v_x$  is the movement velocity of the contact point in the X-axis direction, with the unit of m/s,  $v_y$  is the movement velocity of the contact point in the Y-axis direction, with the unit of m/s,  $v_z$  is the movement velocity of the contact point in the Z-axis direction, with the unit of m/s. According to the analysis of Figure 3 and Formula (3), the key factor that

affects the lifting of sugarcane is velocity  $v_x$ . To successfully raise the LS, it is necessary to satisfy the velocity  $v_x < 0$ . Studies have shown that a reasonable speed for the lifting scrolls is 160 r/min [32], and the FV of the harvester is usually 1~3 km/h under the condition of sugarcane lodging. In addition, the relative position of the LS and the crop dividers lifter may also be a key factor affecting the quality of sugarcane [31].

## 2.2. Sugarcane Lodging Levels

The relative position of the crop dividers and the LS is shown in Figure 4, where  $\alpha$  and  $\theta$  represent the side angle and the lodging angle, respectively. The side angle  $\alpha$  is the angle between the LS and the forward direction of the crop dividers, and the lodging angle  $\theta$  is the angle between the sugarcane projection on the YOZ plane and the horizontal plane. Based on the values of side angles, the sugarcane lodging can be divided into five categories: forward lodging ( $\alpha = 0^\circ$ ), side and forward lodging ( $0^\circ < \alpha < 90^\circ$ ), side lodging ( $\alpha = 90^\circ$ ), side and inverse lodging ( $90^\circ < \alpha < 180^\circ$ ), and reverse lodging ( $\alpha = 180^\circ$ ). Based on the values of lodging angle, the sugarcane lodging can be divided into three categories: slight lodging ( $\theta \geq 60^\circ$ ), medium lodging ( $30^\circ \leq \theta < 60^\circ$ ) and severe lodging ( $0^\circ \leq \theta < 30^\circ$ ) [18]. The actual lodging forms of sugarcane in the field are mainly side and forward lodging, side and inverse lodging, and side lodging. It has always been a difficult issue in sugarcane research to improve LS smoothly [23].

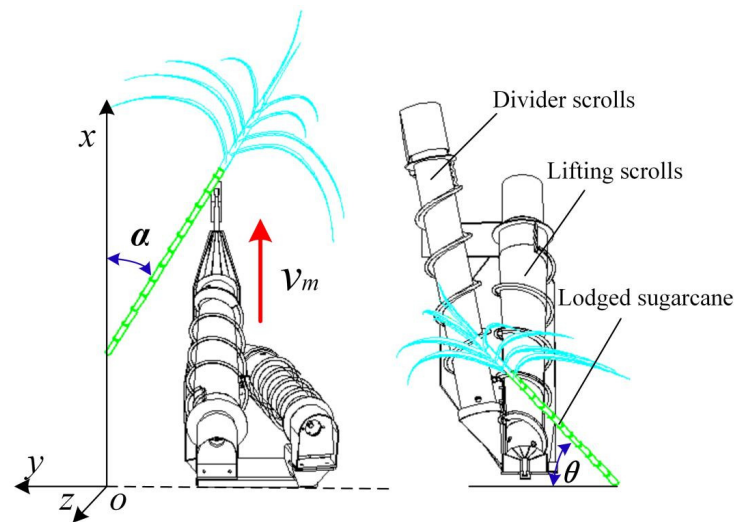


Figure 4. Schematic diagram of sugarcane lodging angle.

## 3. Establishing System Dynamics and Simulation Design

### 3.1. Rigid-Flexible Coupling Modeling

To make the simulation test close to the real operating state of the mechanism, it is crucial to carry out digital dynamics modeling [33–35]. We used the rigid-flexible coupling method to build a simulation model, which can accurately predict the motion characteristics between the crop dividers and the sugarcane. The sugarcane model is built as a flexible body, and the crop dividers model is built as a rigid body. Building the flexible sugarcane creates hybrid coordinates to describe the position change and elastic deformation of the sugarcane. We can obtain the flexible generalized coordinates on the sugarcane model:

$$\xi = \{X, \Psi, q\}^T = \{x, y, z; \alpha, \theta, \gamma; q_m\}^T \quad (4)$$

The position vector of any node  $p$  on the sugarcane is expressed as:

$$r_i^p = r_i + A \left( s_i^p + u_i^p \right) \quad (5)$$

where  $A$  is coordinate transformation matrix;  $u_i^p$  is the elastic deformation of node  $p$ ;  $r_i$  is position coordinate matrix of floating base node;  $s_i^p$  is position in Cartesian coordinate system of node  $i$ .

The coupled motion process is a composite motion of rigid body motion and elastic deformation. Therefore, the basic theory of multi-rigid body dynamics and the basic theory of flexible body dynamics are combined to obtain the system dynamics equations of rigid-flexible coupling as:

$$\begin{cases} \frac{d}{dt} \left( \frac{\partial L}{\partial \dot{\zeta}} \right) - \frac{\partial L}{\partial \zeta} + \frac{\partial \Gamma}{\partial \dot{\zeta}} + \left[ \frac{\partial \Psi}{\partial \dot{\zeta}} \right]^T = Q \\ \Psi = 0 \end{cases} \quad (6)$$

where  $\Psi$  is constraint equation,  $\lambda$  is a Lagrange multiplier of  $\Psi$ ,  $Q_g$  is the generalized force projected onto  $\zeta$ ,  $L$  is Lagrange term,  $T$  is kinetic energy,  $W$  is potential energy,  $\Gamma$  is energy loss,  $\zeta$  is generalized coordinates of flexible bodies,  $M$  is flexible mass matrix,  $K$  is generalized stiffness matrix of generalized coordinates, and  $D$  is generalized damping matrix of generalized coordinates.

The kinetic energy of the flexible body is:

$$T = \frac{1}{2} \dot{\zeta}^T M(\zeta) \dot{\zeta} \quad (7)$$

The potential energy of the flexible body is:

$$W = W_g(\zeta) + \frac{1}{2} \zeta^T K \zeta \quad (8)$$

$$L = T - W \quad (9)$$

The gravity of an object is:

$$G = \int_0^V g \rho r_i dV = \int_0^V g \rho \left[ x + A(A(s_{i0}^p + u_i^p)) \right]^T dV \quad (10)$$

The generalized forces generated by gravity is:

$$Q_g = \frac{\partial G}{\partial \zeta} \quad (11)$$

where  $G$  is gravity of object,  $V$  is volume of object,  $g$  is the acceleration of gravity,  $A$  is the acceleration of gravity, and  $\rho$  is the material density. Combining the above equations yields.

$$M\ddot{\zeta} + \dot{M}\dot{\zeta} - \frac{1}{2} \left[ \frac{\partial M}{\partial \zeta} \dot{\zeta} \right]^T \dot{\zeta} + K\zeta + f_g + D\dot{\zeta} + \left[ \frac{\partial \Psi}{\partial \dot{\zeta}} \right]^T \lambda = Q_g \quad (12)$$

Before establishing the rigid-flexible coupling simulation model, the crop dividers were appropriately simplified, the lifting scrolls, the crop divider toes and the bracket were retained, and CATIAV5R20 (Dassault Aviation, Biard, France) software was used to establish a three-dimensional model, saving it in .stp format. The .stp file was imported into the ADAMS2019 (MSC.Software, Newport Beach, CA, USA) software, three flexible sugarcane stalks were selected, and the root contact set with the ground as a spherical hinge. In addition, the motion attributes were set for the crop dividers model. The model building process is shown in Figure 5, and the relevant input parameters are shown in Table 1 [32,36,37].

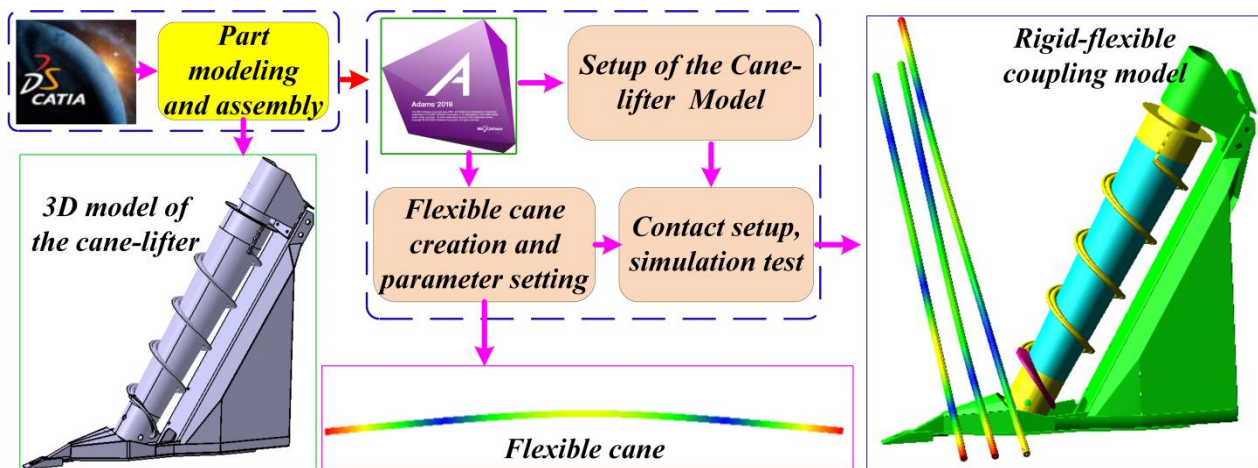


Figure 5. Rigid-Flexible Coupling Simulation Model.

Table 1. Types and values of simulation model parameters.

Parameters	Values
Length of lifting scrolls/mm	1300
Pitch/mm	250
Inclination angle between lifting scrolls and horizontal plane/°	60
Length of sugarcane stalk/mm	3000
Diameter of sugarcane stalk/mm	30
Distance between adjacent sugarcane/mm	125
Poisson's ratio	0.33
Elastic modulus/(N·mm <sup>-2</sup> )	1195.44
Distribution density/(kg·mm <sup>-3</sup> )	$1.1 \times 10^{-6}$
Stiffness/(N/mm)	2855
Force exponent	1.1
Maximum damping N/(m/s)	0.57
Penetration depth/mm	0.1
Static coefficient	0.30
Dynamic coefficient	0.25
Stiction transition velocity/(mm/s)	0.10
Friction transition velocity/(mm/s)	10.00

### 3.2. Simulation Design

Consistent with the analysis of LS in Section 2, this article takes severe LS ( $0^\circ \leq \theta < 30^\circ$ ) as the research object and chooses a lodging angle of  $15^\circ$ . Sugarcane stalks with forward lodging and reverse lodging have no contact with the crop divider during the harvesting operation, so they are outside the scope of the study [25]. The lodging postures of sugarcane were selected as side and forward lodging, side lodging, side and inverse lodging, and the side angles were respectively  $30^\circ$ ,  $60^\circ$ ,  $90^\circ$ ,  $120^\circ$  and  $150^\circ$ . Referring to the relevant studies conducted by [12], the FV of the harvester was selected as 1 km/h, 2 km/h, and 3 km/h, and the experimental analysis under different conditions was carried out.

According to practical needs and existing research, sugarcane height variation is an important indicator for describing the lifting efficiency [23]. To clearly observe the height variation pattern of LS during the lifting process, the change trend and average maximum value of the VHC in the process of sugarcane lifting were selected as evaluation indicators. The VHC of the sugarcane is shown in Figure 6. The sugarcane was set to be homogeneous, with the midpoint coinciding with the centroid. The calculation is as follows:

$$h = \frac{H}{2} \sin \theta \quad (13)$$

where  $h$  is VHC of sugarcane, with the unit of mm, and  $H$  is total length of the sugarcane, with the unit of mm.

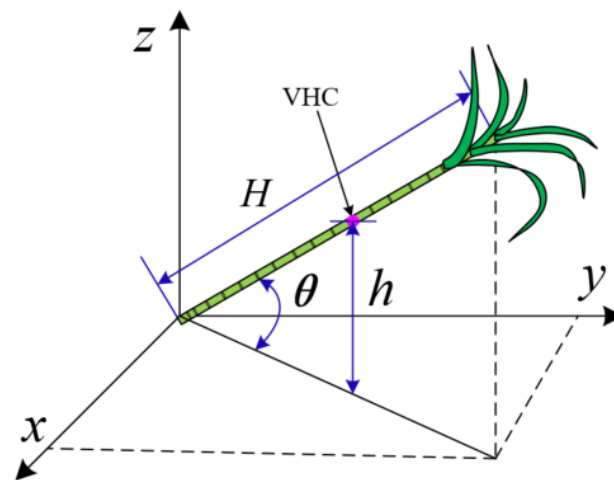


Figure 6. Calculation of VHC.

## 4. Results and Discussion

### 4.1. Validation Test

To verify the accuracy of the simulation model, a field verification experiment was carried out during the sugarcane harvest season in 2020, in Daxu Village, Laibin City, and Guangxi Province, as shown in Figure 7. Ratoon sugarcane was selected for the experiment, variety Guiliu 136. The average height was about 2860 mm, and the planting density was 8 roots/m. In the field validation test, it was difficult to obtain the position change of the sugarcane centroid at different times. Therefore, the maximum height average value of the midpoint of the sugarcane in each group of tests was selected as the evaluation index. During the test, the FV of the harvester was selected to be 2 km/h, and the sugarcane was selected to be in severe lodging. The side angles were approximately  $30^\circ$ ,  $60^\circ$ ,  $90^\circ$ ,  $120^\circ$  and  $150^\circ$ . The experimental results are shown in Table 2. It can clearly be seen that the maximum error rate between the simulation and experimental results was 8.84%, and the minimum error was 3.53%. Errors in the test were unavoidable, including random errors caused by parameter settings, uneven ground in the field, and variable speed control of the harvester driver. After calculation, the average error rate was 5.41%. We believe that the simulation model established by the rigid-flexible coupled method is accurate.



Figure 7. Field validation tests.

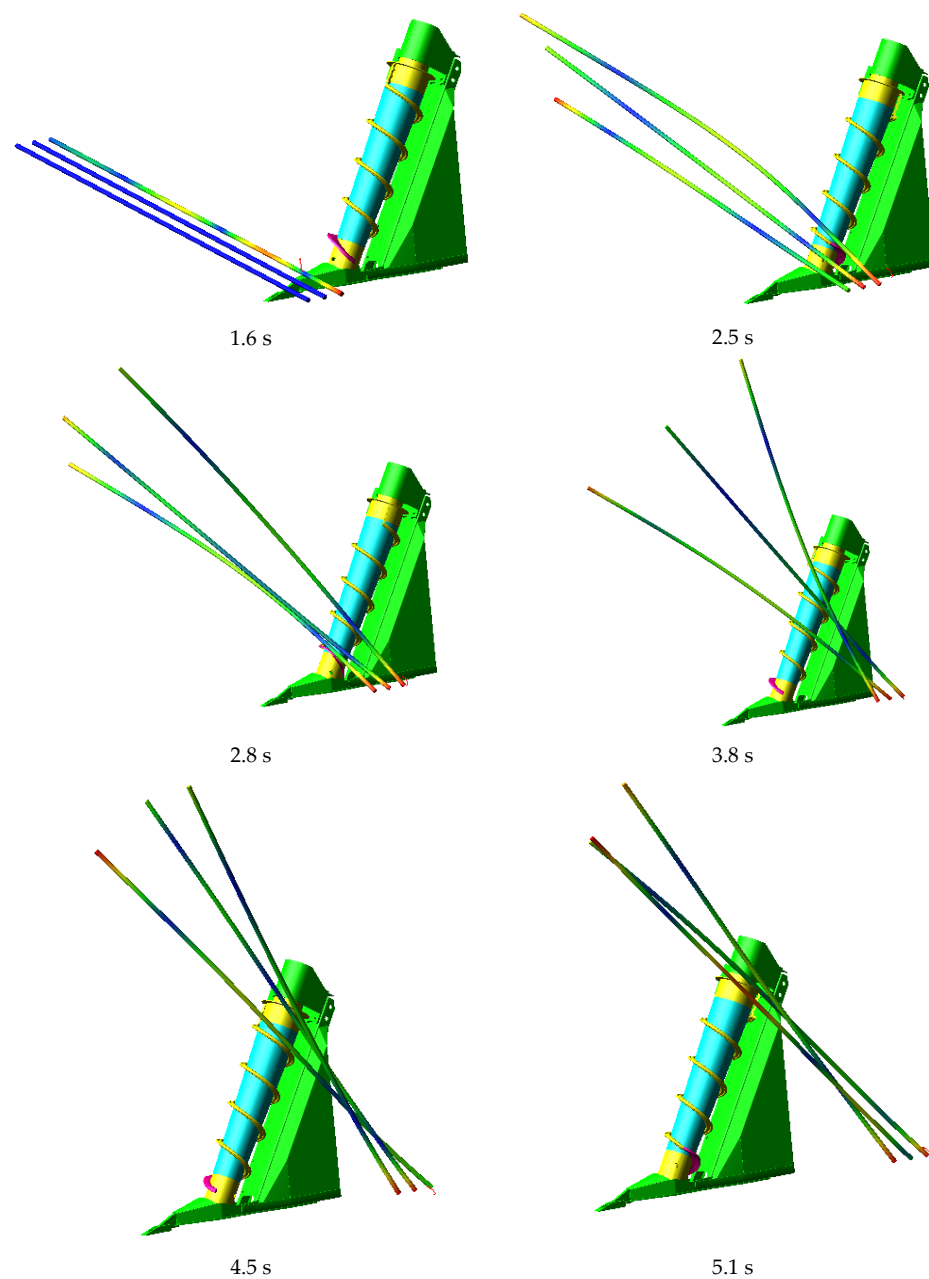


**Table 2.** Comparison of simulation and field test results.

Side angles	30°	60°	90°	120°	150°
Test values/mm	757	1082	1263	1401	1417
Simulation values/mm	810	1145	1342	1463	1467
Error rate/%	7.00	5.82	8.84	4.43	3.53

#### 4.2. Analysis of the Lifting Process of LS

To observe the lifting change of the sugarcane stalk, the FV was 2 km/h and the sugarcane posture was side lodged ( $\alpha = 90^\circ$ ). The interaction screenshots at different moments were analyzed, as shown in Figure 8. According to the contact sequence of the sugarcane and the lifting scrolls, the three sugarcanes were numbered #1, #2 and #3, respectively.

**Figure 8.** LS lifting process.

It can be seen from Figure 8 that over 1.6~2.5 s, with the operation of the crop dividers, the LS first contacts the crop dividers toes, and is slightly lifted, and then moves to the spiral guide plate under the rotation of the scrolls. The sugarcane gradually moves along the spiral guide plate to the spiral guide tubes. In 2.8~3.8 s, the sugarcane rises along the spiral guide tubes, and the LS height gradually increases. It can also be observed that, during this time period, #2 sugarcane had the lowest height during the lifting process due to the interaction between the sugarcane and the divider. From 4.5 to 5.1 s, it was found that with continuous operation of the crop dividers, the posture of the LS gradually changed from side lodging to side and forward lodging. When the three sugarcanes were gradually lifted to the upper end of the lifting scrolls, they stayed on the upper end of the scrolls for a time. During this period, the height of the sugarcane did not change significantly, which is more conducive to the cutting of the sugarcane by the cutter. The sugarcane bends during the whole process of being lifted, which is consistent with what occurs during field operations.

#### 4.3. Change in VHC of LS

Figures 9–11 show the change curve of VHC during the lifting process of the LS under the conditions of FV 1, 2 and 3 km/h, and side angles of 30°, 60°, 90°, 120° and 150°. The slope of the rising trend of the curve in the figure indicates the rising speed of VHA during the lifting process.

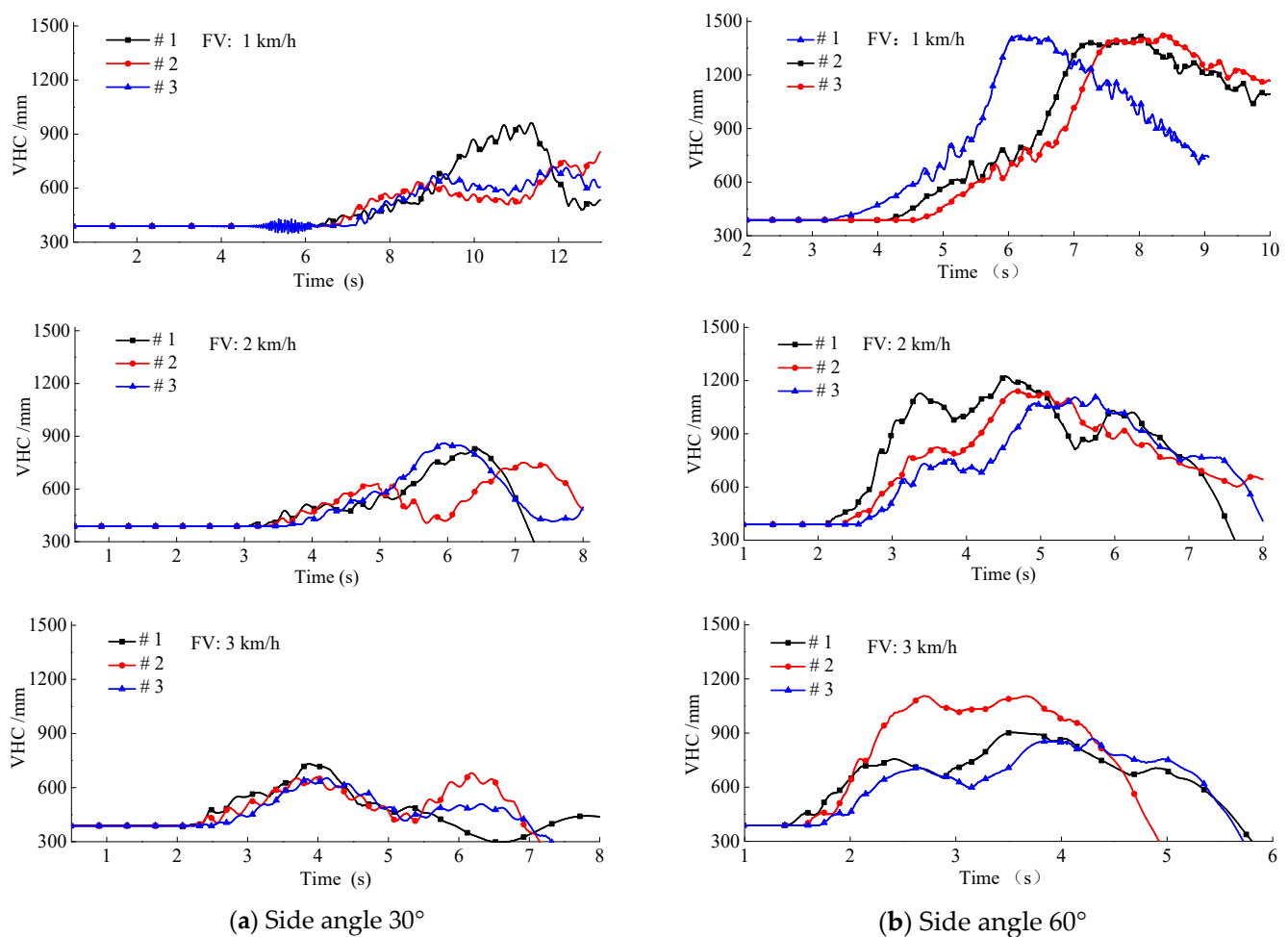


Figure 9. Change of VHC in side and forward LS.

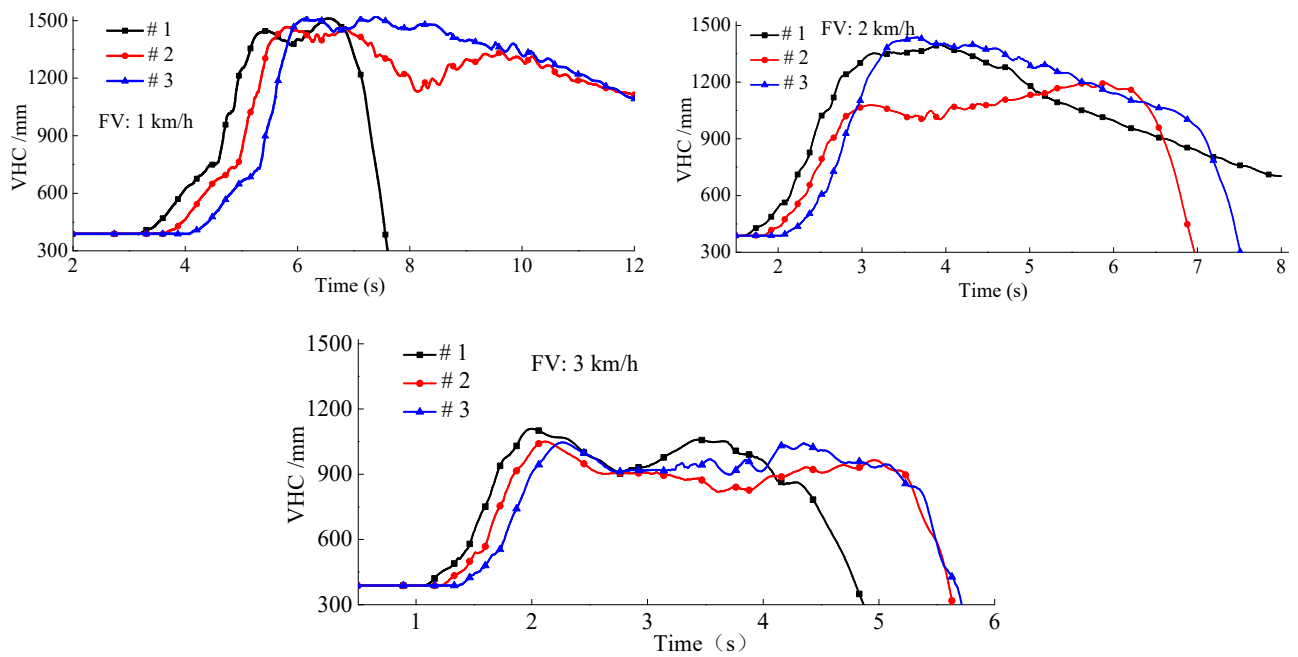
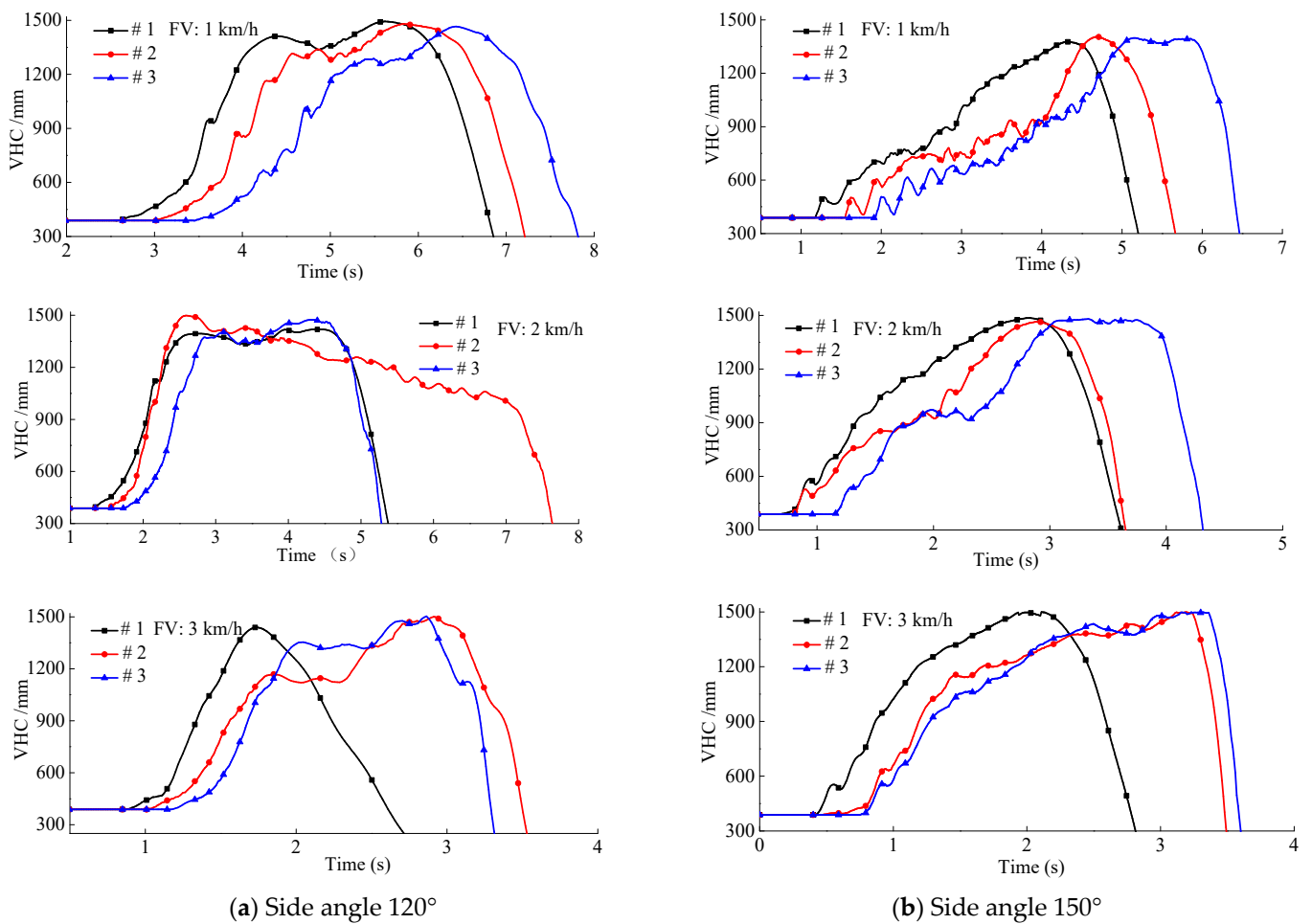


Figure 10. Change of VHC in side LS.



(a) Side angle 120°

(b) Side angle 150°

Figure 11. Change of VHC in side and inverse LS.

Figure 9 shows the change curve of sugarcane VHC during the process of being lifted under conditions of side and forward lodging. The curve presents a fluctuating trend that first rises and then falls, and the curves of each group of experiments have concave points, which all indicate that the sugarcane is prone to slipping during the lifting process. It can also be observed in Figure 9a that as the FV increases, the time for the LS to reach the maximum height gradually shortens, and the maximum lifted height gradually decreases. When the FV is 2 km/h, the uniformity of the maximum VHC is improved.

Figure 9b shows the change curve of the VHC during the lifting process under different FV with a slip angle of  $60^\circ$ . As the FV increases, the value of the maximum VHC gradually decreases. When the FV is 1 km/h, the speed at which the VHC is raised is relatively slow, and when the VHC rises to about 700 mm, the curve will fluctuate. When the FV is 2 km/h and 3 km/h, VHC will descend after reaching the first wave crest, and most of the sugarcane will slide when it is lifted about 720 mm, and then slowly lifted again.

The VHC curve of side angle  $60^\circ$  can be compared with side angle  $30^\circ$ : the curve fluctuation is smoother, the frequency of sugarcane slipping in the process of lifting has significantly reduced, and the speed of fallen sugarcane in the process of lifting has increased. When the FV is the same, the time to lift the VHC of the fallen sugarcane to its maximum value decreases and the height increases.

Figure 10 shows the change curve of VHC during the lifting process of side LS. As the FV increases, the maximum value of VHC is gradually reduced, which is significantly higher than that of side and forward lodging. According to the curve, the crop dividers can quickly lift the LS, and as the FV increases, the time to be raised to the maximum height gradually decreases. In addition, the sugarcane can be maintained at the maximum height for a long time, and no slipping occurs during the lifting process.

Figure 11 shows the change curve of VHC during the raising process of the sugarcane in the side and reverse lodging posture. According to Figure 11a, at the lateral declination angle of  $120^\circ$ , it can be seen that the difference of the maximum value of VHC at different FV is small. At an FV of 1 km/h, the VHC is lifted slowly and smoothly, reaches its maximum height with the operation of the crop dividers, maintains it for a period of time, and then gradually drops. At FV of 2 and 3 km/h, the time taken for the LS to be lifted to its maximum height was comparable. At a FV of 2 km/h, the change in VHC is close to the same for the three sugarcanes during the rising process.

In Figure 11b a side angle of  $150^\circ$  can be obtained, with increase in FV the time sugarcane is held up is gradually increased, the time to reach the maximum height gradually becomes smaller, while the difference in the maximum value of VHC is minimal. The change curve of VHC gradually smooths out with increase in FV, which indicates that the increase in FV was conducive to the rapid and smooth lifting of sugarcane in the side and reverse lodging posture.

The interaction between the variation pattern of VHC and the side angles is significant, as can be observed from Figures 9–11. There are two sugarcanes with more similar trends for different side angles. The interaction between the variation pattern of VHC and the side angles is significant. The time for VHC to be lifted to the maximum height tends to decrease as the FV increases. From the trend of slope change of VHC curve during lifting of LS, the magnitude of lifting speed during lifting of sugarcane with different lodging postures is: side lodging > side and inverse lodged > side and forward lodged. When the side angles are  $90^\circ$  and  $120^\circ$ , the change curve of fallen sugarcane VHC is smoother than other side angles, indicating that the sugarcane can be lifted more smoothly and not easily slip. The frequency of sugarcane slipping in different lodged postures was: side and forward lodged > side and inverse lodged > side lodged.

#### 4.4. Analysis of the Average Value of the Maximum VHC

Shown in Figure 12 are the average values of the maximum VHC lifted by the spiral crop dividers for three severely LS ( $\theta = 15^\circ$ ) under different FV and different side angles.

The X-axis in the figure is the FV, the Y-axis is the side angles, and the Z-axis is the average value of the maximum VHC for each sugarcane.

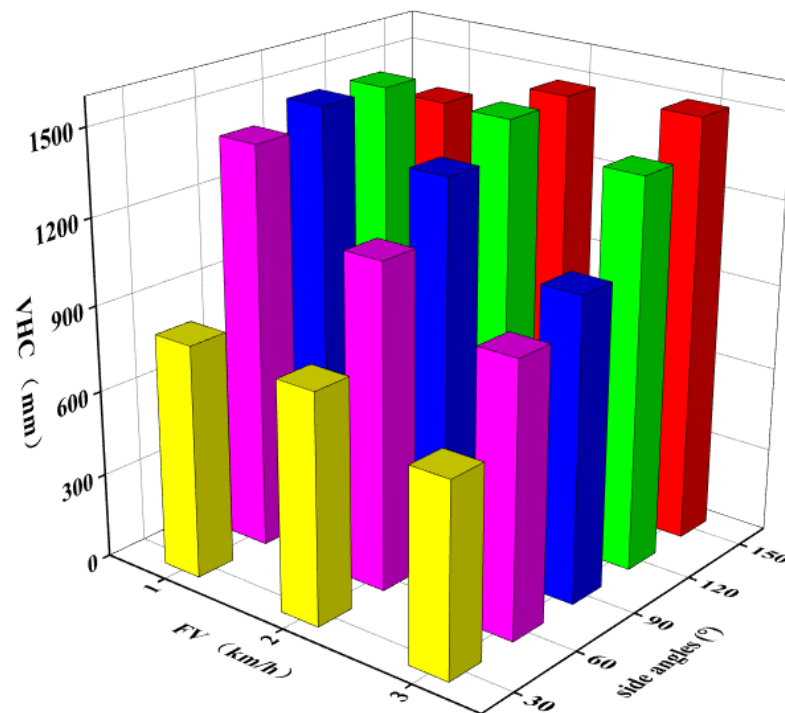


Figure 12. Average value of maximum VHC.

Figure 12 shows that when the FV is 2 km/h and 3 km/h, the VHC of the sugarcane being lifted gradually increases as the side angles increase. Under the exact condition of FV, the average maximum value of VHC is the lowest when the side angle is 30°, and the variation range of the maximum value is the smallest.

The available literature has not found a clear distinction as to when the height of the sugarcane lift meets requirements. To measure whether the height of LS being lifted meets the requirements, this paper takes the lodging angle of 45° as the dividing line; when the lodging angle is greater than 45° this indicates that the lifting height meets the performance requirements and the lifting height of sugarcane is qualified. According to Equation (13) calculation, the critical value of lifting qualified sugarcane VHC is 1.06 m.

It can be determined from Figure 12 that the maximum average height of sugarcane VHC lifted at different FV is significantly higher than the qualified value with side and inverse lodging. When the sugarcane was side lodged, the average value of maximum VHC was 1068.53 mm at the FV of 3 km/h, which was slightly higher than the qualified value. When the sugarcane is in side and forward lodging, only when the side angle is at 60° and the FV is at 1 km/h and 2 km/h, does the average value of maximum VHC reaches the qualified standard.

Based on the analysis in Section 4.2 and Section 4.3, the recommended FV for harvesting at different side angles when the sugarcane is severe lodged, taking into account the speed of VHC lifting, the uniformity of the maximum height and the frequency of slipping, is as follows: when the side angle is about 30°, it is more appropriate to choose an FV of 2 km/h; when the side deviation angle is about 60° and 90°, it is more appropriate to choose an FV of 1 or 2 km/h; when the FV is 120° and 150°, it is more appropriate to choose an FV of 2 or 3 km/h. This can also inform the selection of the proper operating speed for unmanned sugarcane harvesters to reduce the loss rate during harvesting of LS.

To improve the lifting efficiency of severe LS, it is also essential to choose a reasonable sugarcane lodged position during harvester operation. According to the experimental analysis in this paper, the preferential selection of sugarcane's lodged posture is in the following order: side and reverse lodged > side lodged > side and forward lodged.

## 5. Conclusions

This paper introduces different categories of sugarcane lodging by side angles and lodging angles, establishes a simulation model of LS and spiral crop divider using the rigid-flexible coupling method, and verifies the accuracy of the model by field tests.

The test results showed that with increase in FV the time of sugarcane being lifted to the maximum height showed a decreasing trend. The slipping frequency was greatest during lifting side and forward LS, especially when the side angle was about 30°. When the side angle was about 90° and 120°, the LS lifted most smoothly and rapidly. According to the analysis of the lifting speed and passing rate of VHC, the recommended choice of LS posture during the operation of the harvester is: side and reverse lodged > side lodged > side and forward lodged.

This coupled simulation approach can be applied to many applications to analyze mechanical systems to improve the efficiency and reliability of the system. Finally, as possible future work, we anticipate further optimizing the design of crop dividers to explore more precise operating parameters, providing initial conditions and parameter configurations for future coordinated operation between unmanned harvesters in smart agriculture.

**Author Contributions:** Conceptualization, L.C.; methodology, Q.W.; software, Q.W.; validation, Q.Z.; formal analysis, Y.Z.; investigation, G.Z.; resources, L.C.; data curation, Q.W.; writing—original draft preparation, Q.W.; writing—review and editing, L.C.; supervision, Z.L.; project administration, Q.W.; funding acquisition, L.C. All authors have read and agreed to the published version of the manuscript.

**Funding:** This study was funded by the Collaborative Innovation Project of Colleges and Universities of Anhui Province (Grant No. GXXT-2020-011) and Anhui Province Science and Technology Major Projects (Grant No. 18030701194).

**Institutional Review Board Statement:** Not applicable.

**Informed Consent Statement:** Not applicable.

**Data Availability Statement:** The data presented in this study are available on request from the corresponding author.

**Conflicts of Interest:** The authors declare no conflict of interest.

## References

1. Sunil, K.M.; Tony, E.G.; Alan, C.H. Effect of blade oblique angle and cutting speed on cutting energy for energy cane stems. *Biosyst. Eng.* **2015**, *133*, 64–70.
2. Rajan, B.; Jagdish, S.; Alison, M.L.; Ram, S.M.; Walaa, F.A.; Ahmed, G.; Akbar, H. Potassium and Water-Deficient Conditions Influence the Growth, Yield and Quality of Ratoon Sugarcane (*Saccharum officinarum* L.) in a Semi-Arid Agroecosystem. *Agronomy* **2021**, *11*, 2257.
3. Salassi, M.E.; Breaux, J.B.; Naquin, C.J. Modeling within-season sugarcane growth for optimal harvest system selection. *Agric. Syst.* **2002**, *73*, 261–278. [[CrossRef](#)]
4. Phoonthawee, S.; Nattinee, S.; Kamonthip, S. Sequential Injection System for Analysis of Degree Brix, Orthophosphate and pH in Raw Sugarcane Juice Applicable to Sugar Industry. *Molecules* **2021**, *26*, 6484.
5. Wang, F.; Ma, S.; Xing, H.; Bai, J.; Ma, J.; Yang, Y.; Hu, J. Base cutting energy consumption for sugarcane stools using contra-rotating basecutters. *Trans. ASABE* **2021**, *64*, 221–230. [[CrossRef](#)]
6. Stray, B.J.; Vuuren, J.H.; Bezuidenhout, C.N. An optimization-based seasonal sugarcane harvest scheduling decision support system for commercial growers in South Africa. *Comput. Electron. Agric.* **2012**, *83*, 21–31. [[CrossRef](#)]
7. Kallaya, K.; Supachai, P. Integrating a multiple crop year routing design for sugarcane harvesters to plant a new crop. *Comput. Electron. Agric.* **2017**, *136*, 58–70.
8. Mathanker, S.K.; Gan, H.; Buss, J.C.; Lawson, B.; Hansen, A.C.; Ting, K.C. Power requirements and field performance in harvesting energycane and sugarcane. *Biomass Bioenergy* **2015**, *75*, 227–234. [[CrossRef](#)]
9. Lucas, A.S.G.; Rouverson, P.S.; Patricia, C.M.; Fanciele, M.C.; Cristiano, Z.; Antonio, T.S.O. Quality of multi-row harvesting in sugarcane plantations established from pre-sprouted seedlings and billet. *Ind. Crop. Prod.* **2019**, *142*, 111831.
10. Ou, Y.; Malcolm, W.; Yang, D.; Liu, Q.; Zheng, D.; Wang, M.; Liu, H. Mechanization technology: The key to sugarcane production in China. *Int. J. Agric. Biol. Eng.* **2013**, *6*, 1–27.
11. Xie, L.; Wang, J.; Cheng, S.; Zeng, B.; Yang, Z. Optimisation and finite element simulation of the chopping process for chopper sugarcane harvesting. *Biosyst. Eng.* **2018**, *175*, 19–26. [[CrossRef](#)]

12. Xing, H.; Ma, S.; Wang, F.; Bai, J.; Ma, J. Aerodynamic Performance Evaluation of Sugarcane Harvester Extractor Based on CFD. *Sugar Tech* **2021**, *23*, 627–633. [[CrossRef](#)]
13. Song, C.; Ou, Y. Design and Simulation Analysis of Two-stage Conical Helical Sugarcane Support Mechanism. *J. Agric. Mech. Res.* **2019**, *41*, 137–141, 147.
14. Yang, W.; Zhao, W.; Liu, Y.; Chen, Y.; Yang, J. Simulation of forces acting on the cutter blade surfaces and root system of sugarcane using FEM and SPH coupled method. *Comput. Electron. Agric.* **2021**, *180*, 105893. [[CrossRef](#)]
15. Marcelo, A.S.; Lucas, A.H.; Maria, M.P.S.; Gabriel, H.G.; Alexandrius, M.B.; Leandro, B. Base Cut Quality and Productivity of Mechanically Harvested Sugarcane. *Sugar Tech Int. J. Sugar Crop. Relat. Ind.* **2020**, *22*, 284–290.
16. Deng, J.; Li, S.; Liang, S. Conceptual design and innovation on holding device of sugarcane harvester. *Trans. Chin. Soc. Agric. Mach.* **2003**, *34*, 58–61.
17. Cortez, J.W.; Missio, C.; Barreto, A.K.G.; Silva, M.D.D.; Reis, G.N. Quality of sugarcane mechanized planting. *Eng. Agric.* **2016**, *36*, 1136–1144. [[CrossRef](#)]
18. Bai, J.; Ma, S.; Wang, F.; Xing, H.; Ma, J.; Wang, M. Performance of Crop Dividers with Reference to Harvesting Lodged Sugarcane. *Sugar Tech* **2020**, *22*, 812–819. [[CrossRef](#)]
19. Mou, X. *Design and Test on the Rake Bar Chain-Type Sugarcane Lifter*; South China Agricultural University: Guangzhou, China, 2008.
20. Bai, J.; Ma, S.; Wang, F.; Xing, H.; Ma, J.; Hu, J. Field test and evaluation on crop dividers of sugarcane chopper harvester. *Int. J. Agric. Biol. Eng.* **2021**, *14*, 118–122. [[CrossRef](#)]
21. Gao, J.; Ou, Y. Theoretical study on spiral sugarcane lifting mechanism of sugarcane harvester and virtual prototype simulation. *Trans. Can. Soc. Assoc. Exec.* **2004**, *20*, 1–5.
22. Gao, J.; Ou, Y.; Song, C.; Zhang, Y.; Qing, S. Study on Virtual Prototype of Spiral Sugarcane-lifting Organ Based on Physical Model. *Trans. Confocal Scanning Acoust. Microsc.* **2005**, *36*, 57–59.
23. Song, C.; Ou, Y.; Liu, Q.; Wang, M. Experimental study on influencing factors of lifting quality for push-over-type sugarcane harvester. *Trans. Can. Soc. Assoc. Exec.* **2012**, *28*, 35–40.
24. Song, C.; Ou, Y. Lifting effect of spiral sugarcane-lifting mechanism. *J. Hunan Agric. Univ.* **2004**, *30*, 569–571.
25. Song, C.; Ou, Y.; Liu, Q.; Xie, F. Simulation and experiments of two-stage spiral sugarcane picking-up mechanism. *Trans. Can. Soc. Assoc. Exec.* **2011**, *27*, 106–110.
26. Dong, Z.; Meng, Y.; Li, Y. Design of non-equidistant pitch sugarcane propping device. *J. Agric. Mech. Res.* **2010**, *32*, 80–84.
27. Xie, F.; Ou, Y.; Liu, Q. Experiment of Combined-lifter Device for Sugarcane Harvester. *Trans. Confocal Scanning Acoust. Microsc.* **2011**, *42*, 94–98.
28. Duan, T.; Wei, J.; Zhang, A.; Xu, Z.; Teik, C.L. Transmission error investigation of gearbox using rigid-flexible coupling dynamic model: Theoretical analysis and experiments. *Mech. Mach. Theory* **2021**, *157*, 104213. [[CrossRef](#)]
29. Xia, H.; Zhen, W.; Chen, D.; Zeng, W. Rigid-flexible coupling contact action simulation study of the open mechanism on the ordinary multilayer fruit paper bag for fruit bagging. *Comput. Electron. Agric.* **2020**, *173*, 105414. [[CrossRef](#)]
30. Liu, F.; Huang, H.; Li, B.; Hu, Y.; Jin, H. Design and analysis of a cable-driven rigid-flexible coupling parallel mechanism with variable stiffness. *Mech. Mach. Theory* **2020**, *153*, 104030. [[CrossRef](#)]
31. De Paula Corrêdo, L.; Canata, T.F.; Maldaner, L.F.; de Jesus Alves de Lima, J.; Molin, J.P. Sugarcane Harvester for In-field Data Collection: State of the Art, Its Applicability and Future Perspectives. *Sugar Tech* **2021**, *23*, 1–14. [[CrossRef](#)]
32. Hu, J.; Wang, J.; Hu, Y. Optimization of parameters for sugarcane lifter based on simulation of virtual prototype. *J. Zhejiang Univ.* **2014**, *40*, 111–118.
33. Yang, T.; Bai, Z.; Li, Z.; Feng, N.; Chen, L. Intelligent Vehicle Lateral Control Method Based on Feed forward + Predictive LQR Algorithm. *Actuators* **2021**, *10*, 228. [[CrossRef](#)]
34. Chen, L.; Li, Z.; Yang, J.; Song, Y. Lateral Stability Control of Four-Wheel-Drive Electric Vehicle Based on Coordinated Control of Torque Distribution and ESP Differential Braking. *Actuators* **2021**, *10*, 135. [[CrossRef](#)]
35. Chen, L.; Ma, P.; Tian, J.; Liang, X. Prediction and optimization of lubrication performance for a transfer case based on computational fluid dynamics. *Eng. Appl. Comput. Fluid Mech.* **2019**, *13*, 1013–1023. [[CrossRef](#)]
36. Zhang, Z.; Jia, X.H.; Yang, T.; Gu, Y.L.; Wang, W.W.; Chen, L.Q. Multi-objective optimization of lubricant volume in an ELSD considering thermal effects. *Int. J. Therm. Sci.* **2021**, *164*, 106884. [[CrossRef](#)]
37. Xie, L.; Wang, J.; Cheng, S.; Zeng, B.; Yang, Z. Optimization and dynamic simulation of a conveying and top breaking system for whole-stalk sugarcane harvesters. *Biosyst. Eng.* **2020**, *197*, 156–169. [[CrossRef](#)]